Power Electronic Systems
Laboratory

Proceedings of the 22nd IEEE International Industrial Technology Conference (ICIT 2021), Valencia, Spain,
March 10-12, 2021

Modular Multilevel Converter Circulating Current Control with Single Active Filter Module per Phase

J. Huber,
J. W. Kolar

Eidgenössische Technische Hochschule Zürich
Swiss Federal Institute of Technology Zurich

Modular Multilevel Converter Circulating Current Control with Single Active Filter Module per Phase

Jonas E. Huber and Johann W. Kolar
Power Electronic Systems Laboratory, ETH Zurich
Physikstrasse 3, 8092 Zurich, Switzerland
huber@lem.ee.ethz.ch
www.pes.ee.ethz.ch

***Abstract*—Phase-legs of DC/AC modular multilevel converters (MMC, M2LC) transfer power from the DC input to the corresponding phase output terminal by means of a current that circulates through the DC input and the phase-leg. In addition to the load-dependent DC component required for the power transfer, this circulating current contains significant harmonics if no countermeasures are implemented. Prominently, a large second harmonic appears, essentially because each converter arm performs a single-phase power conversion. This results in higher RMS values of the arm currents and ultimately in higher-than-necessary losses. One option to mitigate these undesired harmonics and the associated losses extends each arm of the MMC by an active filter module that controls the circulating current by injecting a common-mode component into the arm voltage. In this paper, we propose a new variant of an MMC topology with such active filter modules. In contrast to the state of the art, the proposed realization shows lower realization effort: it uses only a single active filter module per MMC phase-leg instead of two, which corresponds to a reduced effort in terms of both, power hardware components and also control and communication electronics. Furthermore, a single active filter module can operate fully self-contained if desired, i.e., without an external communication interface, thus simplifying system integration.**

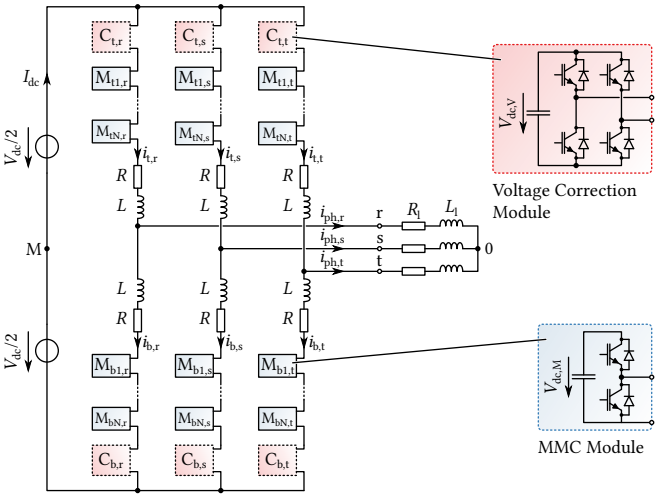

Fig. 1. DC/AC modular multilevel converter (MMC, M2LC) topology with a passive load. Each converter arm consists of several half-bridge MMC modules. In addition, the topology features optional voltage correction modules as proposed in [8], [9] to control the circulating current, see Sect. I-B for details.

I. Introduction

The modular multilevel converter (MMC, M2LC) as proposed in 2002 by Marquardt et al. [1] [2], building on earlier concepts involving chains of converter modules [3], is a modular, scalable multilevel topology that is suitable for various applications involving high power and high voltage levels such as HVDC transmission or large medium-voltage drive systems; see [4], [5] for an overview. **Fig. 1** shows a typical configuration of a three-phase DC/AC MMC.

A. Operating Principle of the MMC

Literature discusses the functionality of the MMC topology in great detail. For example, [6] describes the operating principle very clearly. Therefore and for the sake of conciseness, we give a brief overview only.

Each of the MMC's phase-legs consists of an upper and a lower converter *arm*. Each arm comprises N converter modules and an arm inductor, L, whereby the DC voltage of one converter module amounts to $V_{\mathrm{dc,M}} = V_{\mathrm{dc}}/N$ (note that the sum of the module DC voltages of a single arm equals the total DC voltage if no redundancy of modules is considered).

The typically employed half-bridge modules (see **Fig. 1**) can assume two switching states: *inserted*, i.e., the arm current flows through the module's DC-side capacitor and hence the capacitor voltage appears between the module's output terminals, or *bypassed*, i.e., the arm current flows though the module's low-side switch and the terminal voltage is ideally zero. By inserting and bypassing a certain number of modules per arm, e.g., using phase-shifted carrier pulse-width modulation (PWM) [7], each arm behaves as a controlled voltage source (cf. the equivalent circuits in **Fig. 2**).

Thus, the potential of a phase-leg's output terminal with respect to the (virtual) midpoint of the DC input voltage, M, can be varied between $+V_{\mathrm{dc}}/2$ and $-V_{\mathrm{dc}}/2$ by inserting and bypassing an appropriate number of modules in the top and bottom arm, respectively. In average, N modules must be inserted per phase-leg to avoid an excessive buildup of circulating current, see also (6) below. As each arm can provide sufficient voltage to balance the total DC input voltage, it is possible to do so for any potential of the output terminal (e.g., if the phase voltage with respect to MP is $+V_{\mathrm{dc}}/2$, none of the top arm's modules is inserted but all of the bottom arm's

modules are inserted).

Active balancing of the modules' DC capacitor voltages is necessary: typically, a sorting-algorithm decides which modules to insert or bypass based on the arm current direction and the modules' capacitor voltages [2].

Following [6], for reasons of symmetry the arm currents are given by

$$i_{\mathrm{t,i}} = i_{\mathrm{circ,i}} + \frac{i_{\mathrm{ph,i}}}{2} \qquad \text{and} \qquad i_{\mathrm{b,i}} = i_{\mathrm{circ,i}} - \frac{i_{\mathrm{ph,i}}}{2}, \quad (1)$$

where $i = \mathrm{r,s,t}$; note that we omit the subscript "$_\mathrm{i}$" in the following when referring to an arbitrary MMC phase-leg. Thus, the arm currents contain a component of the phase current but also a circulating current, i_{circ}, that flows in the loop spanned by the main DC-bus and the phase-leg's two arms. Ideally, this circulating current contains a DC component only, i.e.,

$$i_{\mathrm{circ}} = \frac{I_{\mathrm{dc}}}{3}, \quad (2)$$

which is sufficient to maintain the energy balance between the DC and the AC side.

However, without special considerations, i.e., if the top and bottom arm are directly modulated with a sinusoidal reference signal as indicated above, the circulating current contains significant harmonics; most important, a large second harmonic at $2f_{\mathrm{g}}$, i.e., twice the AC-side fundamental frequency, appears (see the first 100 ms of the waveforms shown in **Fig. 8e**). Correspondingly, also the arm currents show harmonic distortions (see **Fig. 8d**) that increase their RMS values and hence the overall converter losses.

Whereas a detailed discussion is beyond the scope of this paper, we briefly outline an intuition for how the second harmonic component forms, using the example of a single-phase MMC as shown in **Fig. 2b**, where the idealized current flows from (1) are indicated. The power processed by the bottom arm of phase-leg r becomes:

$$\begin{aligned} p_{\mathrm{b,r}}(t) &= v_{\mathrm{b,r}}(t) \cdot i_{\mathrm{b,r}}(t) \\ &= \left(\frac{V_{\mathrm{dc}}}{2} + \frac{mV_{\mathrm{dc}}}{2}\sin\omega_{\mathrm{g}}t\right) \cdot \left(\frac{I_{\mathrm{dc}}}{2} - \frac{\hat{i}_{\mathrm{ph}}}{2}\sin\omega_{\mathrm{g}}t\right) \\ &= \frac{V_{\mathrm{dc}}I_{\mathrm{dc}}}{4} + \left(\frac{V_{\mathrm{dc}}I_{\mathrm{dc}}}{4}m - \frac{V_{\mathrm{dc}}\hat{i}_{\mathrm{ph}}}{4}\right) \cdot \sin\omega_{\mathrm{g}}t \\ &\quad \underbrace{-\frac{mV_{\mathrm{dc}}\hat{i}_{\mathrm{ph}}}{4}\sin(\omega_{\mathrm{g}}t)^2} \\ &\quad -\frac{mV_{\mathrm{dc}}\hat{i}_{\mathrm{ph}}}{4}\left(\frac{1}{2} - \frac{1}{2}\cos 2\omega_{\mathrm{g}}t\right), \end{aligned} \quad (3)$$

where $m = \hat{v}_{\mathrm{ph}}/V_{\mathrm{dc}}$ is the modulation index and $\omega_{\mathrm{g}} = 2\pi f_{\mathrm{g}}$. A similar expression can be found for the power processed by the top arm:

$$\begin{aligned} p_{\mathrm{t,r}}(t) = \frac{V_{\mathrm{dc}}I_{\mathrm{dc}}}{4} - \left(\frac{V_{\mathrm{dc}}I_{\mathrm{dc}}}{4}m - \frac{V_{\mathrm{dc}}\hat{i}_{\mathrm{ph}}}{4}\right) \cdot \sin\omega_{\mathrm{g}}t \\ - \frac{mV_{\mathrm{dc}}\hat{i}_{\mathrm{ph}}}{4}\sin(\omega_{\mathrm{g}}t)^2 \end{aligned} \quad (4)$$

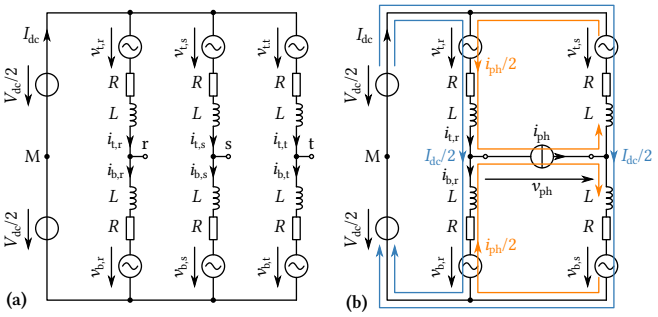

Fig. 2. **(a)** Three-phase DC/AC MMC (cf. **Fig. 1**) equivalent circuit, modeling the arms as controlled voltage sources. **(b)** Equivalent circuit of a single-phase DC/AC MMC to illustrate the formation of a second harmonic component in the currents circulating between the DC input and the phase legs. Note that in the three-phase case, the phase current components of phase r would close their paths through the load star point and both of the other two phase-legs, s and t.

First, note that the DC components in the expressions for the arm powers cancel out, as

$$\frac{mV_{\mathrm{dc}}\hat{i}_{\mathrm{ph}}}{4} \cdot \frac{1}{2} = \frac{\hat{i}_{\mathrm{ph}}\hat{v}_{\mathrm{ph}}}{8} = \frac{1}{4} \cdot \frac{\hat{i}_{\mathrm{ph}}\hat{v}_{\mathrm{ph}}}{2} \stackrel{!}{=} \frac{1}{4}V_{\mathrm{dc}}I_{\mathrm{dc}}, \quad (5)$$

i.e., in time average, the energy stored in the arm's capacitors remains constant. Second, $p_{\mathrm{b,r}}(t)$ and $p_{\mathrm{t,r}}(t)$ each contain a component at *twice* the grid frequency because each arm essentially performs a single-phase power conversion. These components are *in phase*. As the module's capacitances are finite, a voltage fluctuation must arise in both arms that thus drives a corresponding second harmonic in the circulating current through the two arm inductors (see also (6) below). In contrast, the power components at the grid frequency are of opposite phase in the top and bottom arm and thus do not ultimately drive a corresponding harmonic in the circulating current. Further analysis becomes involved quickly as the fluctuating capacitor voltages will in turn impact the power flows etc. Thus, we refer interested readers to the literature, e.g., [11].

B. Circulating Current Control Methods

Literature describes several control strategies to suppress this undesired harmonic content of the circulating current. In general, a common-mode (CM) voltage component of the arm voltages, i.e., $v'_{\mathrm{t}} = v_{\mathrm{t}} + \delta v$ and $v'_{\mathrm{b}} = v_{\mathrm{b}} + \delta v$, adjusts the current through *both* arm inductors, i.e., the circulating current, since

$$V_{\mathrm{dc}} - (v'_{\mathrm{t}} + v'_{\mathrm{b}}) = 2L \cdot \frac{\mathrm{d}i_{\mathrm{circ}}}{\mathrm{d}t} \quad (6)$$

(neglecting the small series resistances, R). Note that this CM component does not affect the phase-leg's output voltage because

$$v_{\mathrm{ph}} = \frac{v'_{\mathrm{t}} - v'_{\mathrm{b}}}{2} + \frac{L}{2} \cdot \left(\frac{\mathrm{d}i_{\mathrm{b}}}{\mathrm{d}t} - \frac{\mathrm{d}i_{\mathrm{t}}}{\mathrm{d}t}\right) \quad (7)$$

(again neglecting R and with v_{ph} referring to the voltage between the MMC phase-leg output terminal and the input DC-bus midpoint, M.)

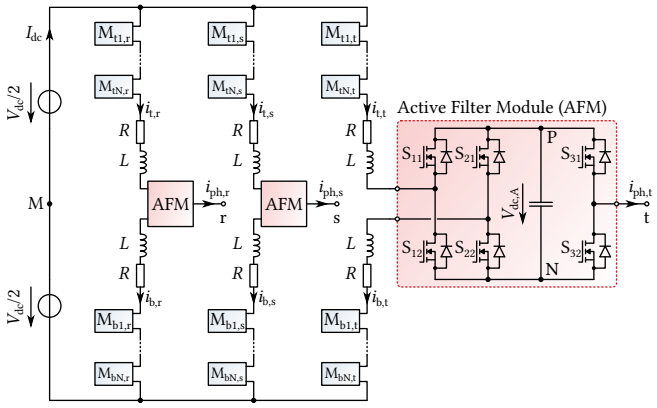

Fig. 3. Proposed simplified topology using only a single active filter module (AFM) per MMC phase-leg instead of two voltage correction modules as shown in **Fig. 1**).

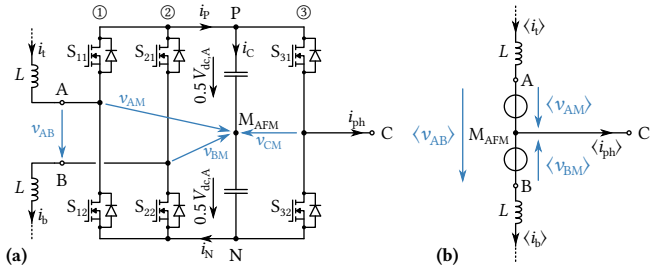

Fig. 4. **(a)** Power circuit schematic of the AFM, indicating a (virtual) midpoint, $\mathrm{M_{AFM}}$, of its DC bus. **(b)** Equivalent circuit (local average values with respect to one AFM switching period, $T_{\mathrm{s,A}}$). Note that $\langle v_{\mathrm{CM}} \rangle = 0$ because bridge-leg ③ operates with a duty ratio of 50 %.

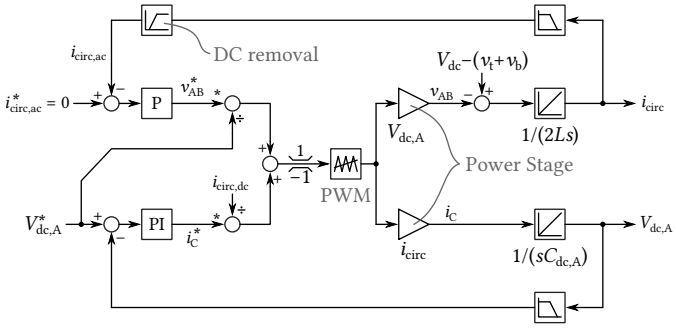

Fig. 5. AFM control diagram. The upper control loop regulates the AC component of the circulating current to zero, the lower feedback loop ensures a stable AFM DC-bus voltage (note that $i_{\mathrm{circ,dc}}$ can be obtained as $i_{\mathrm{circ,dc}} = i_{\mathrm{circ}} - i_{\mathrm{circ,ac}}$). The proportional gain of the circulating current controller must be negative because of the chosen definition of v_{AB}. All quantities refer to local average values, yet to simplify the notation, the triangular braces ($\langle x \rangle$) are omitted. Furthermore, we neglect minor delays introduced by the measurements, sampling, the PWM modulator, and the power stage, considering the required control bandwidths.

The most straightforward solution [6] adds these CM components to the arm voltages by adapting the modulation signals, i.e., directly with the MMC modules. However, doing so requires a sufficient voltage reserve. Seen from another perspective, the phase output voltage capability for a given DC voltage decreases. This is typically not an issue in systems with a larger number of modules, since these anyway often feature additional modules for redundancy purposes.

Recently, Madawala and Riar have proposed an alternative approach that employs dedicated voltage correction modules in each arm [8] [9], see **Fig. 1**. These voltage correction modules basically act as active filters that add (CM) components to the arm voltages, i.e., the CM voltage components required for reducing the harmonic content of the circulating current are now added by dedicated converter modules instead of by the MMC modules themselves.

The voltage correction modules can operate with a fraction of an MMC module's DC voltage. Therefore, costs can be lower compared to adding MMC modules that realize the voltage reserve for the control-based circulating current minimization strategy described above. Furthermore, the control of the output current (and hence the phase-leg output voltage) and the control of the circulating current are performed by different entities: the former is performed by the basic MMC structure, the latter by the dedicated voltage correction modules. This full decoupling of the two control tasks can be seen as another advantage. Note that the floating DC bus of a voltage correction module can be supplied through its AC port by suitable control, i.e., there is no need for an external supply to ensure a constant DC-bus voltage of the voltage correction module in an MMC arm.

II. Proposed Circulating Current Control with a Single Active Filter Module

Based on the state-of-the-art solution that features one voltage correction module per arm (see [8], [9] and **Fig. 1**), we propose a simplified realization that requires only a single active filter module (AFM) *per MMC phase-leg* [10]. **Fig. 3** shows the new topology, where the AFM is connected between the arm inductors and the phase-leg output terminal.

The basic operating principle is the same as that of the state-of-the-art topology: the AFM's two bridge-legs connected to the arm inductors can add a CM voltage, v_{AB}, to the arm voltages in order to control the circulating current. The AFM's third bridge-leg operates with a duty ratio of 50 % to virtually connect the phase terminal to the midpoint of the MMC phase-leg, see **Fig. 4**. Furthermore, suitable control can maintain the AFM's DC-bus voltage without the need for an external power supply.

A. Control

The AFM can control the circulating current by adjusting its output voltage, v_{AB}, which appears as a CM voltage on the left-hand side of (6), i.e., $v'_{\mathrm{t}} = v_{\mathrm{t}} + v_{\mathrm{AB}}/2$ and $v'_{\mathrm{b}} = v_{\mathrm{b}} + v_{\mathrm{AB}}/2$. The top part of **Fig. 5** shows the corresponding control loop, which uses a proportional controller (note that also PI or resonant controllers could be used instead [9]). The circulating current can be obtained from measurements of the arm currents as

$$i_{\mathrm{circ}} = \frac{i_{\mathrm{t}} + i_{\mathrm{b}}}{2}, \tag{8}$$

which follows from (1). Low-pass filtering the (indirectly) measured circulating current ensures that the controller does not act on disturbances at the (equivalent) switching-frequency of the MMC. Finally, to fully decouple the AFM operation from the regulation of the converter's output quantities (phase voltages or currents of the three-phase load, active and reactive power, etc.), the AFM suppresses only the AC components of the circulating current (e.g., extracted by means of a high-pass filter), as the DC component changes with the output power. Note that in this mode of operation, the AFM control is fully self-contained (provided the AFM features its own arm current measurements), i.e., in principle there is no need for an external control interface (or only for a very basic interface, e.g., to enable/disable the module). This is in contrast to the state-of-the-art approach where the two voltage correction modules per phase-leg share the total CM voltage generation and hence need to communicate with each other or with a central controller, e.g., because each module has only access to one of the arm currents.

Alternatively, the AFM could be integrated in the overall converter control system and then control the circulating current to an arbitrary reference value, which could be obtained, e.g., from measured output power flows as in [9] or from MMC arm energy balance considerations [6].

A second control loop (see bottom of **Fig. 5**) stabilizes the AFM's DC-bus voltage, essentially by adjusting the output voltage, v_{AB}, such that together with the circulating current a net power flow into or out of the AFM results. Since the circulating current controller ensures $i_{\mathrm{circ}} \approx I_{\mathrm{dc}}/3 = const.$, this amounts to adding a (small) DC component to v_{AB}.

The two control loops can be designed independently using standard design procedures and tools, whereby typically the bandwidth of the DC-bus voltage controller is selected much lower than that of the current controller (e.g., 50 Hz and 500 Hz, respectively, for the example system discussed in Sect. III).

B. Modulation Considerations

The AFMs first two bridge-legs (legs ① and ②, see **Fig. 4**) form a full-bridge that operates with standard unipolar PWM, which can be implemented with two triangular carriers that are phase-shifed by 180° with respect to each other, see **Fig. 6a**. However, as indicated above and in **Fig. 4b**, bridge-leg ③ must operate with 50 % duty ratio to virtually connect the phase output terminal to the midpoint of the two arm inductors, i.e., to render the AFM transparent regarding the output quantities.

Thus, the phase shift of the output leg's modulation signal with respect to the full-bridge carriers remains a degree of freedom. Advantageously, this allows to reduce the current stress of the AFM's DC-bus capacitor. **Fig. 7** shows the four switching states for $v_{\mathrm{AB}} = V_{\mathrm{dc,A}}$ or $v_{\mathrm{AB}} = 0$ and indicates the flow of the arm current components given in (1). Regarding the states POS/P and POS/N, the capacitor current, i_{C}, could be higher in either case depending on the instantaneous value of the phase current. However, during freewheeling of the full-bridge, the state of leg ③ affects

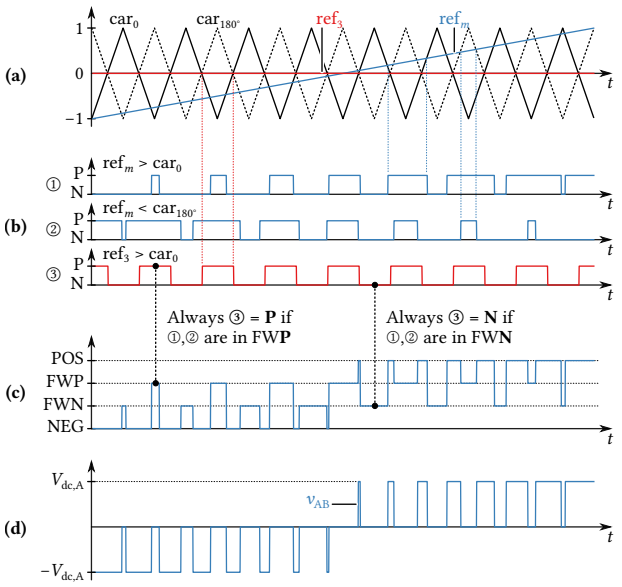

Fig. 6. **(a)** Exemplary unipolar full-bridge modulation with two carriers of opposite phase (car_0 and $\mathrm{car}_{180°}$) and an exemplary reference signal ref_m covering the entire modulation range $m \in [-1, 1]$; the reference signal for leg ③, ref_3, is zero. **(b)** Resulting switching states of the three bridge-legs. **(c)** State of the AFM full-bridge (cf. Fig. 7). **(d)** Resulting AFM output voltage v_{AB}.

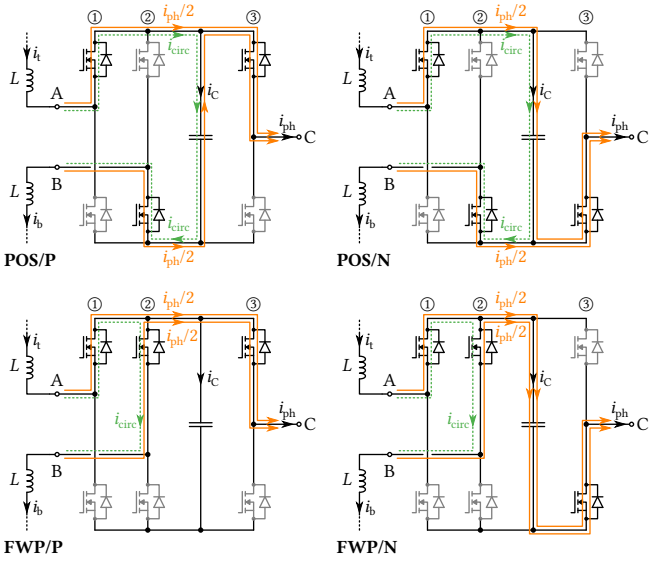

Fig. 7. Exemplary switching states of the AFM (POS: $v_{\mathrm{AB}} = V_{\mathrm{dc,A}}$, FWP: $v_{\mathrm{AB}} = 0$ and upper freewheeling path; the letter after the slash indicates the state of leg ③) and corresponding current flows according to (1). Note that regarding the current stress of the DC-bus capacitor, freewheeling state FWP/P ($i_{\mathrm{C}} = 0$) is clearly preferable to FWP/N ($i_{\mathrm{C}} = i_{\mathrm{ph}}$). The remaining switching states follow from symmetry considerations.

the capacitor current unambiguously: advantageously, only the state FWP/P should be used, as the total phase current would flow through the capacitor in state FWP/N. Equivalent results for $v_{\mathrm{AB}} = -V_{\mathrm{dc,A}}$ follow from symmetry considerations. Overall we find that leg ③ should be modulated such that

TABLE I
SPECIFICATIONS OF THE THREE-PHASE DC/AC MMC EXAMPLE SYSTEM

Parameter		SI		pu
Rated power	S_N	3	MVA	3
Rated voltage (line-to-line)	V_N	4.16	kV	$\sqrt{3}$
Rated phase current	I_N	416	A	1
Output frequency	f_g	50	Hz	
DC voltage	V_dc	8	kV	3.33
Number of MMC modules per arm	N	4		
Module DC voltage	$V_\mathrm{dc,M}$	2	kV	0.83
Module capacitance	$C_\mathrm{dc,M}$	4	mF	7.25
Module switching frequency	$f_\mathrm{s,M}$	1	kHz	
Arm inductance	L	2.7	mH	0.15
Load inductance	L_l	1	mH	0.05
Load resistance	R_l	5.8	Ω	1.01
AFM DC voltage	$V_\mathrm{dc,A}$	400	V	0.17
AFM DC capacitance	$C_\mathrm{dc,A}$	6	mF	10.9
AFM switching frequency	$f_\mathrm{s,A}$	10	kHz	

its state always corresponds to the full-bridge's freewheeling state, i.e., only two of the four possible switching states for freewheeling of the full-bridge should actually be employed: FWP/P and FWN/N. **Fig. 6** illustrates that this is achieved when the modulation signal of leg ③ is in phase with $\mathrm{car}_{180°}$, i.e., leg ③ is in state P if $\mathrm{ref}_3 = 0 > \mathrm{car}_0$. Note that the requirement of 50 % duty ratio for leg ③ prevents further optimization of the capacitor current stress by freely selecting between POS/P and POS/N based on the instantaneous values of i_circ and i_ph.

III. SIMULATION RESULTS

In order to demonstrate the effectiveness of the proposed topology using only a single AFM per MMC phase-leg, we use a detailed simulation model of an exemplary three-phase DC/AC MMC system with specifications given in **Tab. I**.

The AFM's DC voltage is a key design parameter: it should not be too high (to keep switching losses low or to enable high switching frequencies), but it must be high enough for the AFM to apply enough voltage to suitably adjust the circulating current. Thus, a suitable DC voltage of the active filter module can be estimated from the circulating current that would flow without any countermeasures and the corresponding voltage drop across $2L$ at $2f_\mathrm{g}$. Literature describes analytic methods for calculating the harmonic components of the circulating current (e.g., [11] or [12]). However, even approximate expressions are relatively complicated and their validity for specific operating conditions must be checked carefully. Therefore, we use a straightforward approach and determine the voltage drop across the two arm inductors at $2f_\mathrm{g}$ from a simulation as 340 V. Taking into account some voltage reserve for the controllers as well as typical semiconductor blocking voltage ratings, the DC voltage of the AFM can be chosen as low as 400 V, i.e., only 5 % of the application's DC voltage (8 kV) or 20 % of an MMC module's DC voltage (2 kV). The low voltage allows for relatively high switching frequencies, as the switching losses of power semiconductors reduce with blocking voltage. Note

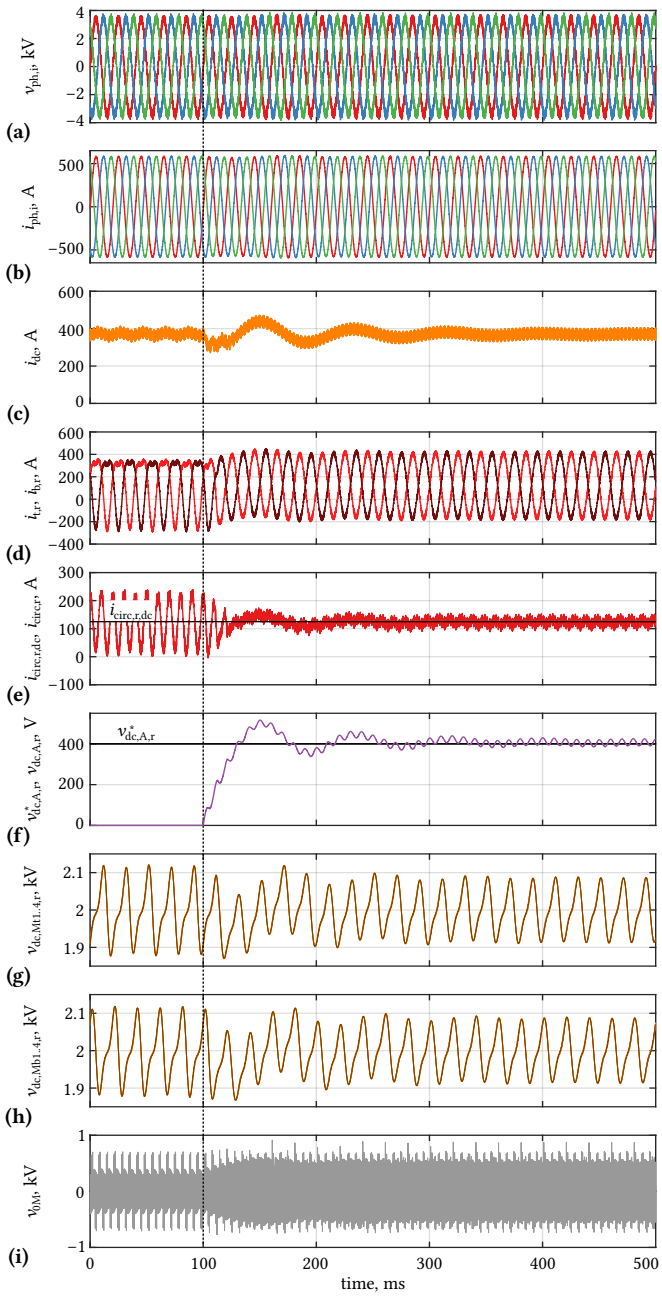

Fig. 8. Key waveforms of the proposed topology shown in Fig. 3; the active filter modules are activated at $t = 100$ ms. **(a)** load phase voltages, **(b)** load phase currents, **(c)** DC input current, **(d)** phase r arm currents, **(e)** phase r circulating current, **(f)** phase r AFM DC bus voltage, **(g)** and **(h)** phase r top and bottom module DC voltages, **(i)** voltage between load star point and input DC-bus midpoint.

that even lower AFM DC voltages would still allow to control the circulating current, as can be verified by simulations; however, considering 400 V DC voltage and a typical blocking voltage utilization of 60 %…70 %, 600 V or 650 V power semiconductors could be used. In this voltage class, rugged power modules with high current ratings are readily available.

Fig. 8 shows simulated key waveforms. Upon activation of the AFMs at $t = 100$ ms, the PI regulator quickly charges the

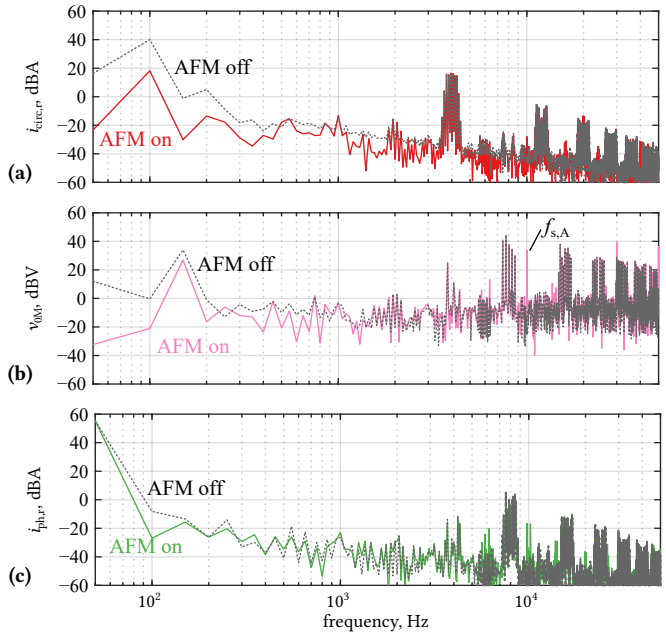

Fig. 9. Effect of the AFM operation on the harmonic content of **(a)** the circulating current, **(b)** the CM voltage between the load star point, 0, and the DC-bus midpoint, M, and **(c)** the load phase currents. The AFM reduces the second harmonic component in the circulating current by more than 20 dBA (i.e., by more than a factor of 10). Note further that the AFM operation does not affect the high-frequency part of the spectra of the output-side quantities (i.e., $i_{\mathrm{ph,r}}$ and $v_{0\mathrm{M}}$) in a way that would necessitate a higher filtering effort.

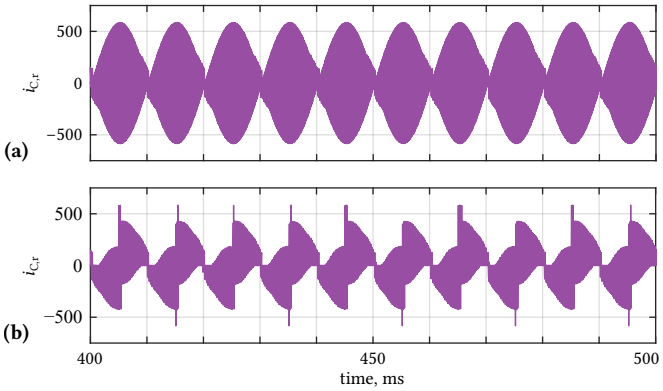

Fig. 10. Simulated AFM (MMC phase R) DC-bus capacitor current, $i_{\mathrm{C,r}}$, where **(a)** leg ③ operates in phase with car_0 and **(b)** leg ③ operates in phase with $\mathrm{car}_{180°}$. The capacitor RMS current reduces from 361 A in **(a)** to 143 A (ca. −60 %) in **(b)**. See also Fig. 6 and Fig. 7.

TABLE II
SIMULATED AFM SEMICONDUCTOR RMS CURRENT STRESS; ARM AND PHASE CURRENT RMS VALUES SHOWN FOR REFERENCE

Device	Legs ①, ②	Leg ③
MOSFET	170 A	291 A
Arm (i_{t}, i_{b})	240 A	
Phase output (i_{ph})	411 A	

AFM's DC capacitor to its nominal voltage; note that the residual voltage fluctuation in steady-state could be further reduced by increasing the AFM's DC-bus capacitance. The AFM then suppresses low-frequency harmonics in the circulating current, i.e., controls it to a DC value, without affecting the output voltages and currents (note the passive resistive-inductive load, see **Tab. I**, i.e., the MMC operates in open-loop as a voltage source). Furthermore, the arm currents change to their ideal sinusoidal shape, causing a reduction of their RMS values by about 4 %, which translates to a 8 % reduction of ohmic losses. Note further that the active control of the circulating current also reduces the voltage ripple of the MMC modules' DC voltages.

Fig. 9 shows the spectra of key converter currents and voltages. The AFM reduces the second harmonic component of the circulating current (at $2f_{\mathrm{g}} = 100$ Hz) by more than 20 dBA, i.e., by more than a factor of 10 (cf. **Fig. 9a**). Since the AFMs of all three MMC phase-legs are operated synchronously, also the CM voltage between the load star point, 0, and M, the (virtual) midpoint of the MMC's DC-bus, $v_{0\mathrm{M}}$, contains harmonics at the switching frequency of the AFM, see **Fig. 9b** and the waveform in **Fig. 8i**. Finally, **Fig. 9c** confirms an only minor impact on the phase current's high-frequency harmonics. All in all, since the AFM's DC-bus voltage, $V_{\mathrm{dc,A}}$, is small compared to an MMC module's DC-bus voltage, $V_{\mathrm{dc,M}}$, and because of the high AFM switching frequency, the harmonics caused by the basic MMC operation dominate the filter attenuation required to meet certain harmonic limits; the operation of the AFMs does not necessitate significant additional filtering effort.

Finally, **Fig. 10** illustrates how an appropriate selection of the phase shift of the modulation signal of leg ③ reduces the RMS current stress of the AFM's DC capacitor from 361 A to 143 A, i.e., by about 60 %. In this context, **Tab. II** lists the RMS currents flowing in the MOSFETs of the AFM (assuming synchronous rectification, i.e., no diode conduction). For reference, the table lists also the RMS values of the arm and the phase currents for the considered full-load operating point of the MMC, where the steady-state AFM modulation index is about 0.53 (at $2f_{\mathrm{g}}$). Note that the device RMS currents of Leg ③ equal $i_{\mathrm{ph}}/\sqrt{2}$, which is the expected result considering the 50 % duty ratio operation of that bridge-leg. Because of the low blocking voltage requirement of only about 600 V (for the selected nominal DC voltage of 400 V), a wide variety of suitable power semiconductors exists, e.g., [13]. Note also that the choice of the AFM switching frequency is subject to a trade-off between losses on the one hand and control bandwidth and additional EMI filtering effort on the other hand. Considering **Fig. 9**, the AFM switching frequency could be lower than the exemplary value of 10 kHz (e.g., 8 kHz or 4 kHz) without affecting the filtering effort. Such a system-level analysis and optimization of efficiency and filtering effort is an interesting direction for future research.

IV. CONCLUSION

Without countermeasures, the current circulating between the DC input and a phase-leg of a modular multilevel con-

verter (MMCs) contains undesired harmonics, especially a second harmonic (with respect to the output frequency). These harmonics increase the RMS value of the circulating current above its ideal DC value, which ultimately results in increased losses.

MMC systems with a large number of converter modules typically feature redundant MMC modules and hence sufficient voltage reserve to directly control the circulating current in the two arm inductors by generating common-mode (CM) voltage components with the top and the bottom arm of a phase-leg, respectively [6]. Another state-of-the-art method [8], [9] suppresses the undesired harmonics of the circulating current by means of dedicated voltage correction modules that also add CM components to the two arm voltages to control the circulating current. This approach advantageously fully decouples the control of the circulating current from that of the MMC's output quantities. Furthermore, typically a relatively low voltage suffices to regulate the circulating current, i.e., the correction modules can be realized with a relatively low DC voltage (with respect to the MMC modules), which facilitates higher switching frequencies, smaller size and ultimately lower cost.

In this paper we propose a conceptually similar but simplified implementation, which requires only a single voltage correction, i. e., active filter module (AFM), per MMC phase-leg. Thus, the proposed solution requires only three instead of four bridge-legs, only one instead of two DC-bus capacitors (although with twice the DC voltage for similar performance), and only one set of control and communication electronics per MMC phase-leg. Furthermore, a single AFM per phase can operate fully self-contained, i.e., rely on its own arm current measurements to control the circulating current to zero. Hence, there is no need for an external communication interface to exchange high-bandwidth signals such as measurement data or controller set points etc. However, an enable/disable input and a status output may be useful; also, an auxiliary power supply is still required. This, together with the connection of the AFM at the phase terminals (instead of in the MMC arms) facilitates straightforward integration and possibly even retrofitting.

Considering reliability, the AFM may be seen as a possible single point of failure, as there is no redundancy. However, the MMC can operate without the AFM (i.e., after short-circuiting a failed AFM; practical realizations could feature corresponding bypassing switchgear), albeit with non-ideal circulating current and hence higher component stresses. As discussed above, these increases of the stresses are moderate, i.e., likely tolerable until repair of the AFM, especially when considering typical design margins.

Thus, extensions of the MMC topology by dedicated active filter modules such as the one proposed here should be seen as a means of improving the converter performance, especially in cases where a decoupled control of the circulating current is desirable, e.g., in MMC systems with only few modules. For such applications, the proposed solution is an interesting option due to its simplicity and the comparably low effort in terms of additional hardware.

REFERENCES

[1] R. Marquardt, A. Lesnicar, and J. Hildinger, "Modulares Stromrichterkonzept für Netzkupplungsanwendungen bei hohen Spannungen (in German)," Proc. ETG Fachtagung, Bad Nauheim, Germany, 2002.

[2] A. Lesnicar and R. Marquardt, "A new modular voltage source inverter topology," Proc. 10th Europ. Power Electron. and Appl. Conf. (EPE), Toulouse, France, Sep. 2003.

[3] R. H. Baker, "Electric power supply," U.S. Patent 3,971,976, July 1976.

[4] M. A. Perez, S. Bernet, J. Rodriguez, S. Kouro, and R. Lizana,"Circuit topologies, modeling, control schemes, and applications of modular multilevel converters," *IEEE Trans. Power Electron.*, vol. 30, no. 1, pp. 4–17, Jan. 2015, doi: 10.1109/TPEL.2014.2310127.

[5] S. Debnath, J. Qin, B. Bahrani, M. Saeedifard, and P. Barbosa, "Operation, control, and applications of the modular multilevel converter: A review," *IEEE Trans. Power Electron.*, vol. 30, no. 1, pp. 37–53, Jan. 2015, doi: 10.1109/TPEL.2014.2309937.

[6] A. Antonopoulos, L. Ängquist, and H.-P. Nee, "On dynamics and voltage control of the modular multilevel converter," Proc. 13th Europ. Power Electron. and Appl. Conf. (EPE), Barcelona, Spain, 2009.

[7] B. Li, R. Yang, D. Xu, G. Wang, W. Wang, and D. Xu, "Analysis of the phase-shifted carrier modulation for modular multilevel converters," *IEEE Trans. Power Electron.,* vol. 30, no. 1, pp. 297–310, Jan. 2015, doi: 10.1109/TPEL.2014.2299802.

[8] U. K. Madawala and B. S. Riar, "Modular multi-level converters," U.S. Patent Appl. 2015/0288287 A1, Oct. 2015.

[9] B. S. Riar and U. K. Madawala,"Decoupled control of modular multilevel converters using voltage correcting modules," *IEEE Trans. Power Electron.,* vol. 30, no. 2, pp. 690-698, Feb. 2015, doi: 10.1109/TPEL.2014.2313613.

[10] J. W. Kolar and J. E. Huber, "Modularer Multilevel-Stromrichter (in German)," Swiss Patent Appl. CH 713 723 A2, Apr. 26, 2017.

[11] K. Ilves, A. Antonopoulos, S. Norrga, and H.-P. Nee, "Steady-state analysis of interaction between harmonic components of arm and line quantities of modular multilevel converters," *IEEE Trans. Power Electron.,* vol. 27, no. 1, pp. 57–68, Jan. 2012, doi: 10.1109/TPEL.2011.2159809.

[12] Q. Tu, Z. Xu, H. Huang, and J. Zhang,"Parameter design principle of the arm inductor in modular multilevel converter based HVDC," Proc. Int. Power System Technology Conf., Hangzhou, China, Oct. 2010, doi: 10.1109/POWERCON.2010.5666416.

[13] Infineon, "FF2MR12KM1: 1200V/2mR 62mm C-Series module with CoolSiC™ Trench MOSFET," Datasheet, 2020.